www.nature.com/aps

Acta Pharmacologica Sinica

ARTICLE

Reducing lipid peroxidation attenuates stress-induced susceptibility to herpes simplex virus type 1

Jing-yu Weng[1,2], Xin-xing Chen[1,2], Xiao-hua Wang[1,2], Hui-er Ye[1,2], Yan-ping Wu[1,2], Wan-yang Sun[1,2], Lei Liang[1,2], Wen-jun Duan[1,2], Hiroshi Kurihara[1,2], Feng Huang[3], Xin-xin Sun[4], Shu-hua Ou-Yang[1,2]✉, Rong-rong He[1,2,3]✉ and Yi-fang Li[1,2]✉

Psychological stress increases the susceptibility to herpes simplex virus type 1 (HSV-1) infection. There is no effective intervention due to the unknown pathogenesis mechanisms. In this study we explored the molecular mechanisms underlying stress-induced HSV-1 susceptibility and the antiviral effect of a natural compound rosmarinic acid (RA) in vivo and in vitro. Mice were administered RA (11.7, 23.4 mg·kg^{-1}·d^{-1}, i.g.) or acyclovir (ACV, 206 mg·kg^{-1}·d^{-1}, i.g.) for 23 days. The mice were subjected to restraint stress for 7 days followed by intranasal infection with HSV-1 on D7. At the end of RA or ACV treatment, mouse plasma samples and brain tissues were collected for analysis. We showed that both RA and ACV treatment significantly decreased stress-augmented mortality and alleviated eye swelling and neurological symptoms in HSV-1-infected mice. In SH-SY5Y cells and PC12 cells exposed to the stress hormone corticosterone (CORT) plus HSV-1, RA (100 μM) significantly increased the cell viability, and inhibited CORT-induced elevation in the expression of viral proteins and genes. We demonstrated that CORT (50 μM) triggered lipoxygenase 15 (ALOX15)-mediated redox imbalance in the neuronal cells, increasing the level of 4-HNE-conjugated STING, which impaired STING translocation from the endoplasmic reticulum to Golgi; the abnormality of STING-mediated innate immunity led to HSV-1 susceptibility. We revealed that RA was an inhibitor of lipid peroxidation by directly targeting ALOX15, thus RA could rescue stress-weakened neuronal innate immune response, thereby reducing HSV-1 susceptibility in vivo and in vitro. This study illustrates the critical role of lipid peroxidation in stress-induced HSV-1 susceptibility and reveals the potential for developing RA as an effective intervention in anti-HSV-1 therapy.

Keywords: Herpes simplex virus type 1; stress; corticosterone; arachidonate lipoxygenase 15; phospholipid peroxidation; STING; viral infection; rosmarinic acid; neuronal cells

Acta Pharmacologica Sinica (2023) 44:1856–1866; https://doi.org/10.1038/s41401-023-01095-6

INTRODUCTION

Herpes simplex virus type 1 (HSV-1) is a human neurotropic pathogen widely distributed and transmitted by direct contact. It causes lifelong, recurrent symptoms such as cold sores, keratitis, meningitis, and encephalitis [1–3]. Upon entering the central nervous system (CNS) via trigeminal or olfactory nerves from the site of primary oro-pharyngeal infection, HSV-1 can establish a latent infection in sensory neurons of the trigeminal ganglia [4, 5]. Psychological stress has long been recognized as a major factor in increasing the incidence and severity of HSV-1 infection [6–8]. When stress occurs, the hypothalamic-pituitary-adrenal (HPA) axis is activated, resulting in the release of glucocorticoids, such as corticosterone (CORT) [9, 10]. Although the dominant mechanism remains obscure, this stress hormone has been uncovered to be a major contributor to stress-enhanced HSV-1 infection [6, 10].

The detrimental impact of psychological stress on neurons has become an increasingly pressing concern. The oxidative stress response has long been proposed as a plausible mechanism linking stress to various pathological changes [7, 11, 12]. The accumulation of reactive oxygen species (ROS) has been evidenced in various animal stress models, and a great imbalance of the pro-oxidant/antioxidant ratio has been observed in different organs, particularly brain tissues, of stressed animals [8, 13–15]. In recent years, emerging knowledge on phospholipid peroxidation has garnered much attention due to its critical role as the final executor of ferroptosis, a process involving lipoxygenases-catalyzed oxidation of esterified polyunsaturated carbon chains at the sn-2 position [16]. Excessive phospholipid peroxidation has been implicated in a growing list of physiological and pathophysiological processes, disrupting the host immune response and exacerbating the symptoms of viral infection [17]. Notably, the inhibition of phospholipid peroxidation is essential for maintaining STING-mediated anti-HSV-1 innate immunity [18, 19]. These clues

[1]Guangdong Engineering Research Center of Chinese Medicine & Disease Susceptibility; International Cooperative Laboratory of Traditional Chinese Medicine Modernization and Innovative Drug Development of Chinese Ministry of Education (MOE), College of Pharmacy, Jinan University, Guangzhou 510632, China; [2]Guangdong Province Key Laboratory of Pharmacodynamic Constituents of TCM and New Drugs Research, College of Pharmacy, Jinan University, Guangzhou 510632, China; [3]School of Chinese Materia Medica and Yunnan Key Laboratory of Southern Medicinal Utilization, Yunnan University of Chinese Medicine, Kunming 650500, China and [4]Jiujiang Maternal and Child Health Hospital, Jiujiang 332000, China

Correspondence: Shu-hua Ou-Yang (shouyang@jnu.edu.cn) or Rong-rong He (rongronghe@jnu.edu.cn) or Yi-fang Li (liyifang706@jnu.edu.cn)

These authors contributed equally: Jing-yu Weng, Xin-xing Chen, Xiao-hua Wang.

Received: 11 January 2023 Accepted: 19 April 2023
Published online: 16 May 2023

prompted us to postulate that phospholipid peroxidation may be important in stress-evoked HSV-1 susceptibility.

Rosmarinic acid (RA), an ester of caffeic acid and 3,4-dihydroxy phenyl lactic acid, is commonly found in the *Nepetoideae* subfamily of the *Lamiaceae* and *Boraginaceae* family [20]. This natural compound and its derivatives have been reported to exert protective effects against some viral infections, including hepatitis B virus, influenza, and SARS-CoV-2, but the precise mechanisms remain unknown [21–23]. In the present study, we utilized stress/CORT-established HSV-1 susceptible in vivo and in vitro models and revealed that stress provokes phospholipid peroxidation, thereby rewiring STING-mediated antiviral innate immunity and augmenting HSV-1 infection. Based on this finding, we further clarify that RA maintains the redox balance by directly inhibiting the activity of lipoxygenase 15 (ALOX15) from rescuing stress-dampened innate immunity. Our study establishes a pivotal role for phospholipid peroxidation in stress-induced virus susceptibility and offers a new strategy for HSV-1 therapy.

MATERIALS AND METHODS

Animals and treatments

All animal experiments were approved by the Animal Care and Use Committee of Jinan University (Guangzhou, China). BALB/c male mice (wild type, 4-week-old) were obtained from Guangdong Medical Laboratory Animal Center (Guangzhou, China). *Alox15* male knockout mice were obtained from Jackson Laboratory (Bar Harbor, ME, USA). Mice were maintained under specific-pathogen-free conditions in a controlled environment of 20–22 °C with 50%–70% humidity, and food and water were provided *ad libitum*.

The treatment of animals in BALB/c mice is shown in Fig. 1b. Mice were randomly divided into six groups, including normal control, HSV-1 control, HSV-1 plus stress (model), two doses of RA treatment and Acyclovir (ACV) treatment. To establish the stress model, mice were restrained in a plastic centrifuge tube of 50 mL with holes for 6 h (from 10:00 a.m. to 4:00 p.m.) for 7 consecutive days. On the 7th day, mice were intranasally infected with 5×10^7 PFU/mL of HSV-1 in 20 μL infection medium (DMEM). RA (11.7 or 23.4 mg·kg^{-1}·d^{-1}, i.g.) and ACV (206 mg·kg^{-1}·d^{-1}, i.g.) were administered to mice for a total of 23 days. All mice were sacrificed under pentobarbital sodium anesthesia (45 mg·kg^{-1}; i.p.) after the last treatment of RA or ACV. Animals were sacrificed to obtain plasma and brain tissue for examination. ACV was purchased from Sigma (St. Louis, MO, United States). RA was procured from the National Institutes for Food and Drug Control of China (Beijing, China).

Seven days post-infection, the eye swell score was evaluated as follows: 1, puffy eyelids; 2, puffy eyelids with some crusting; 3, swollen shut with severe crusting; 4, completely swollen shut and crusted over. Symptoms related to neurological disease were scored as follows: 0, normal; 1, jumpy; 2, uncoordinated; 3, hunched/lethargic; 4, unresponsive/no movement. The score of eye infection symptoms was calculated in a blinded manner, according to previous studies by others [24, 25].

Cell culture and primary neuron preparation

SH-SY5Y, PC12, and Vero cells were cultured in DMEM (Gibco, Carlsbad, CA, USA) supplemented with 10% (v/v) FBS (Thermo Fisher Scientific, Rockford, IL, USA), under 5% CO_2 at 37 °C. Primary mouse cortical neurons were prepared as previously described [26]. In brief, the neonatal mice were euthanized, and intact hemispheres were separated from the head. After removing the meninges and hippocampus using a stereoscope, the cortex was dissected and trypsinized in 0.08% trypsin with DNase I (Sigma, St. Louis, MO, USA) for 20 min at 37 °C. Dissociated neuronal cells were cultured in serum-free Neurobasal^{TM} medium (Gibco, Carlsbad, CA, USA) with supplements of 2% B27 (Gibco, Carlsbad, CA, USA), 1% Glutamax (Gibco, Carlsbad, CA, USA) and penicillin and streptomycin. One-half of the medium was replaced with fresh medium twice a week. Primary neurons were used for experiments 11 days after being cultured. All these cells were cultured in DMEM supplemented with 10% fetal bovine serum at 37 °C in 5% CO_2 until 80%–85% confluence.

Cell viability detection by MTT assay

Cells (5000 cells per well) were seeded in 96-well plates, pretreated with RA and CORT (Sigma, St. Louis, MO, United States) for 48 h, and then infected with HSV-1 for 24 h. After treatment, cell viability was detected by the MTT (Sigma, St. Louis, MO, United States) assay according to the manufacturer's instructions.

Western blot analysis

Cells or tissues were resuspended in lysis buffer (Beyotime, Haimen, China) on ice for 30 min, and the supernatants were collected after centrifugation at 13,000 × *g* for 15 min. Protein lysates were separated in 8% or 10% SDS-PAGE and blotted onto PVDF membranes (Millipore Corporation, Billerica, MA, USA). Immunoreactivity was detected with an immobilon^{TM} Western chemiluminescent HRP substrate kit (Fdbio science, Hangzhou, China). GAPDH (FD0063), goat anti-mouse IgG-HRP (FDM007), and goat anti-rabbit IgG-HRP (FDR007) antibodies were purchased from Fdbio Science (Hangzhou, China). ICP27 (ab53480), gB (ab6506), 4-HNE (ab46545), and ALOX15 (ab244205) antibodies were purchased from Abcam (Cambridge, UK). The STING (13647), p-TBK1 (5483), TBK1 (38066), p-IRF3 (37829), IRF3 (4302), and IFN-β (73671) antibodies were purchased from Cell Signaling Technology (Danvers, MA, USA).

Quantitative real-time PCR

Cells or tissues were extracted using the TRIzol reagent (Introvigen, Carlsbad, CA, USA). Total RNA was then reverse-transcribed with a reverse transcription kit (Beijing, China). Quantitative real-time PCR (qRT-PCR) was carried out in triplicate using SYBR Green (Beijing, China) according to the manufacturer's instructions, and fold changes were calculated with the $2^{-\Delta\Delta Ct}$ method. The expression of related genes was normalized to the housekeeping gene 18 S. The primer sequences are listed in Supplementary Table S1.

Virus plaque assays

HSV-1/F strain was propagated and titrated by plaque-forming units (PFU) assay. Briefly, the confluent Vero cells were infected with serial dilutions of HSV-1 and incubated with overlaid DMEM medium supplemented with 2% carboxymethylcellulose and 2% FBS. After 72 h of incubation, the cells were fixed and stained with crystal violet, and the plaques were counted.

Brain tissues were homogenized, thawed, and frozen again. Tissue homogenates were centrifuged at 1300 × *g* for 5 min at 4 °C. The resulting supernatants were collected and added to one well of Vero cell monolayers in 24-well plates seeded the day before. After 2 h incubation, Vero cell monolayers were washed once with PBS, overlaid with medium containing 1% methylcellulose plus 2% FBS for 4 days, and stained to count plaques.

Determination of MDA content, IFN-β level, and ALOX15 activity

Malondialdehyde (MDA) content, interferon-β (IFN-β) level, and ALOX15 activity were determined using commercially available kits according to the manufacturer's instructions. The MDA detection kit was purchased from Nanjing Jiancheng Bioengineering Institute (Nanjing, China). IFN-β ELISA kit was purchased from the R&D system (Minneapolis, MN, USA). ALOX15 inhibition activity was measured using a Lipoxygenase Inhibitor Screening Assay Kit (Cayman Chemical, Ann Arbor, MI, USA).

Co-immunoprecipitation (Co-IP) assay
The STING antibody was incubated with cell lysates to form an antibody/antigen complex in solution at 4 °C overnight. Then, the complex was pulled down from the sample using protein A/G agarose beads (Santa Cruz Biotechnology, Santa Cruz, CA, USA). After that, agarose beads were washed with lysis buffer three times, and the supernatants were analyzed by Western blot analysis.

Flow cytometry analysis
Liperfluo (Dojindo, Kumamoto, Japan) and H_2DCFH (MedChemExpress, Rahway, NJ, USA) staining followed the manufacturer's instructions. Harvested cells were immediately analyzed for potential using a Beckman Coulter Epics XL flow cytometer (Beckman Coulter, Brea, CA, USA).

Liquid chromatography-mass spectrometry (LC-MS)-based phospholipidomics analysis
Lipids were extracted according to the reported Folch procedure [27]. Phospholipids were prepared and analyzed as previously reported [28]. Briefly, phospholipids (PLs) were evaluated by LC-MS utilizing a Dionex Ultimate 3000 HPLC system paired with a Thermo Fisher Scientific Q-Exactive Hybrid Quadrupole-Orbitrap mass spectrometer. PLs were separated on a normal-phase column at a flow rate of 0.2 mL/min (Phenomenex Luna Silica, 3 M, 2.0 mm, Washington DC, USA). The mobile phase consisted of 10 mM ammonium formate in propanol/hexane/water (285:215:5, v/v/v) and 10 mM ammonium formate in propanol/hexane/water (285:215:40, v/v/v). The injection volume was 2 µL. The gradient elution program was set as follows: 0 min, 10% B; 20 min, 32% B; 30 min, 70% B; 32 min, 100% B; 58 min, 100% B; 60 min, 10% B; and 75 min, 10% B.

Phospholipidomics analysis was performed in full MS negative mode (70,000 resolution) and data dependent-MS^2 mode (175,000 resolution). For the MS and MS^2 scans, an isolation window of 1.0 Da was established. Compound Discoverer 2.0 (Thermo Fisher Scientific, Rockford, IL, USA) was used to analyze raw LC-MS data. The *m/z* values were matched within 5 ppm to identify the lipid species. Quantitation of PLs is based on calibration curves generated by internal standards, including CL (16:0/18:2/18:2/20:4), PA (18:1/18:1), PC (18:1/18:1), PE (18:1/18:1), PG (18:1/18:1), PI (18:1/18:1), PS (18:1/18:1)).

Subcellular fractionation
The detailed procedure has been described previously [29]. Cell lysates were collected and resuspended in ice-cold IB cells-1 buffer (225 mM mannitol, 75 mM sucrose, 0.1 mM EGTA, and 30 mM Tris-HCl (pH = 7.4). After gentle homogenization with a Dounce homogenizer (about 200 times), tissue extracts were centrifuged at 600 × *g* at 4 °C for 5 min to obtain the supernatants. After another centrifugation at 600 × *g* for 5 min at 4 °C, the supernatants were removed to a new 50 mL polypropylene tube and centrifuged at 7000 × *g* at 4 °C for 10 min to obtain the crude mitochondrial pellet. The supernatants were centrifuged at 100,000 × *g* at 4 °C for 1 h to get the ER pellet and cytosolic supernatants.

Molecular docking
The Discovery Studio 3.0 docking program was used to verify the binding between compounds and ALOX15. Preparing the protein structure includes adding hydrogen atoms, removing water molecules, and assigning the Charmm forcefield. The CDOCKER algorithm was used to calculate the interaction between compounds and ALOX15.

Microscale thermophoresis (MST) assay
The MST experiment was performed on a Monolith NT.115 Pico using the Monolith Protein Labeling Kit RED-NHS (NanoTemper Technologies GmbH, Munich, Germany). The concentration of RA varied between 15.2 pM–2.5 µM. The experiment was performed at 5% of excitation power and 40% of MST power. MST traces were analyzed at 2.5 s.

Cellular thermal shift assay (CETSA)
Cells were resuspended in a lysis buffer, and cell lysates were aliquoted after centrifugation. RA was added to a final concentration of 200 µM. For the control sample set, the same volume of DMSO was added. Pairs consisting of one control and one experimental sample were heated at different temperatures from 37 to 77 °C for 3 min. The proteins were analyzed by Western blot.

Statistical analysis
All analyses were performed using IBM SPSS Statistics 25.0 (SPSS, Inc., Chicago, IL, USA). One-way ANOVA followed by Dunnett's multiple comparisons tests, one-way ANOVA followed by Tukey's multiple comparisons tests, and a non-parametric Wilcoxon Mann-Whiney U-test were used for statistical analyses. All data are expressed as means ± SD. The *P* values of less than 0.05 are considered statistically significant.

RESULTS

RA alleviates the exacerbation of HSV-1 infection severity induced by stress in mice
Repeated restraint stress was utilized to establish the HSV-1 susceptibility model. Mice were immobilized in a restraint tube daily for 6 h until they were infected with HSV-1 on the 7th day (Supplementary Fig. S1a). Brain tissues were collected to detect the expression of viral-related proteins. Restraint stress was demonstrated to increase the levels of ICP27 and gB proteins (Supplementary Fig. S1b) and *Ul27* and *Ul54* mRNA (Supplementary Fig. S1c, S1d) in the brains of HSV-1-infected mice. Using the stress-provoked HSV-1 susceptibility model, we found that treatment with the natural compound RA significantly reduced stress-augmented mortality (Fig. 1a–c) and alleviated symptoms of eye swelling (Fig. 1d) and neurological disease (Supplementary Fig. S1e). Moreover, RA administration resulted in a reduction in HSV-1 titer (Fig. 1e), as well as viral-related protein and gene expression (Fig. 1f–h). These results altogether suggest the inhibitory effect of RA on stress-induced HSV-1 susceptibility.

RA mitigates CORT-induced susceptibility to HSV-1 infection in vitro
When exposed to stress, the main type of glucocorticoid axis in rodents, CORT, is released into the bloodstream due to the activation of the HPA axis [30–32]. We discovered that treatment with RU486, a glucocorticoid receptor (GR) antagonist, significantly reversed stress-enhanced HSV-1 replication in the brain tissues of mice (Supplementary Fig. S1b, S1c). To further confirm the influence of CORT on HSV-1 infection in neurons, we treated SH-SY5Y cells and PC12 cells with CORT and observed an elevation in the expression of HSV-1 genes and proteins. In comparison, RA treatment demonstrated a concentration-dependent protective effect on cell viability in cells exposed to CORT plus virus (Fig. 2a, b). RA also decreased viral titer in SH-SY5Y (Fig. 2c) and PC12 cells (Fig. 2d). Meanwhile, RA treatment was also observed to inhibit CORT-induced elevation in the expression of viral proteins and genes, including ICP27, gB (Fig. 2e, g), *Ul27* and *Ul54* (Fig. 2f, h).

RA reduces CORT-induced lipid peroxidation
To explore the protective effect of RA on stress-induced HSV-1 susceptibility, we initially examined its influence on the expression of promyelocytic leukemia (PML), an intrinsic immune protein related to stress-provoked HSV-1 susceptibility through its autophagy degradation in our previous study [6]. Unexpectedly, RA treatment failed to affect the stress/CORT-evoked protein

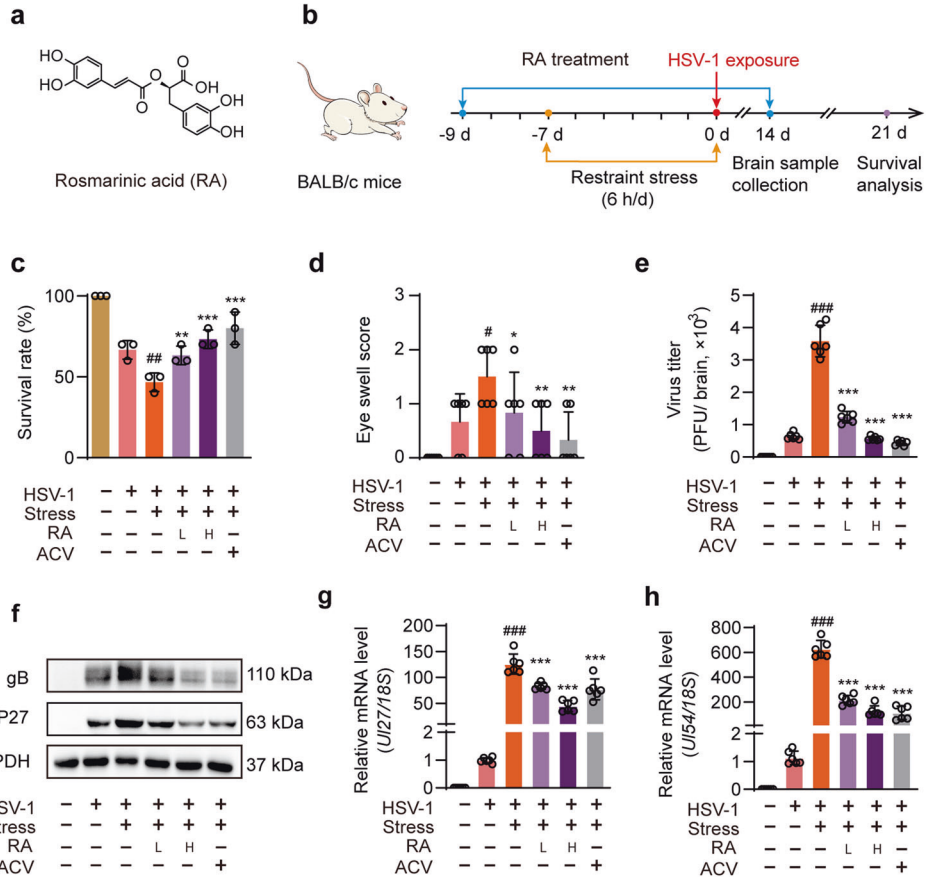

Fig. 1 RA diminishes stress-augmented severity of HSV-1 infection in mice. a Chemical structure of RA. **b** Schematic diagram of stress-established HSV-1 susceptibility and RA treatment (11.7 or 23.4 mg·kg^{-1}·d^{-1}, i.g.). Pathological changes and survival rate were examined on the 14th and 21st days post-infection in mice. **c** The survival rate was monitored for 21 days post HSV-1 infection (three independent experiments with 10 mice per group). **d** Seven days post-infection, the eye swell score was evaluated as follows: 1, puffy eyelids; 2, puffy eyelids with some crusting; 3, swollen shut with severe crusting; 4, completely swollen shut and crusted over ($n = 6$). **e** Virus titer was detected by plaque assay ($n = 6$). **f** The protein expression of ICP27 and gB in the brain tissues was assessed by Western blot analysis. **g**, **h** The mRNA levels of *Ul27* and *Ul54* in the brain tissues were evaluated by qRT-PCR ($n = 6$). Data were presented as mean ± SD. $^{\#}P < 0.05$, $^{\#\#}P < 0.01$, $^{\#\#\#}P < 0.001$ vs. the HSV-1 group; $^{*}P < 0.05$, $^{**}P < 0.01$, $^{***}P < 0.001$ vs. the HSV-1 + stress group.

decline of p62 and PML in the neuronal cells and brain tissues of HSV-1 infected mice (Supplementary Fig. S2a, S2b), indicating another critical target of RA remains to be determined.

Oxidative damage contributes to the susceptibility to various stress-related diseases, including viral infection [33–36]. We monitored the intracellular total ROS level by H_2DCFH probe and found that CORT treatment induced a noticeable ROS accumulation in SH-SY5Y cells (Fig. 3a). Specifically, this stress hormone dramatically increased the level of lipid ROS, indicated by the Liperfluo staining (Fig. 3b). By contrast, RA treatment significantly resulted in a loss of fluorescence intensity of both H_2DCFH and Liperfluo probes (Fig. 3a, b), suggesting that RA may inhibit CORT-induced outburst lipid ROS in cells. In parallel, CORT-caused increases of malondialdehyde (MDA) and 4-HNE, two end-metabolites of lipid peroxidation, were significantly eliminated in SH-SY5Y cells by RA treatment in the absence or the presence of virus (Fig. 3c–f). Meanwhile, RA administration also greatly hindered the stress-induced accumulation of 4-HNE and MDA in the brain tissues of HSV-1-infected mice (Fig. 3g, h). To examine whether the CORT-initiated lipid ROS is derived from the oxidation of polyunsaturated fatty acid (PUFA)-enriched phospholipids (oxPLs) in neurons, we applied liquid chromatography-mass spectrometry (LC-MS/MS) analysis-based phospholipidomics analysis. Notably, CORT significantly increased levels of oxPLs across all species, which were attenuated by RA treatment (Fig. 3i). To dissect the mechanism responsible for the effect of RA on lipid peroxidation, a series of lipid peroxidation-related enzymes were analyzed in CORT-treated SH-SY5Y cells, and the long-chain acyl-CoA synthetase ACSL4 and lipoxygenase ALOX15 were screened out given their considerable alteration at the transcription level (Fig. 3j). We found that knocking down *ACSL4* had a negligible effect on ICP27 expression in cells exposed to CORT and HSV-1. In contrast, si*ALOX15* demonstrated a pronounced reduction in ICP27 expression (Supplementary Fig. S3a, S3b). Restraint stress and CORT treatment up-regulated the protein level of ALOX15 in both the brain tissues of mice (Fig. 3k) and PC12 cells, respectively (Fig. 3l). These observations suggest that the effect of RA on stress-induced viral susceptibility may depend on the regulation of ALOX15-mediated phospholipid peroxidation.

RA maintains redox homeostasis to facilitate STING activation

STING-mediated innate immunity is crucial for sensing cytosolic DNA and initiating TBK1/IRF3/IFN-β signaling against DNA viral infection [37]. Lipid peroxidation has been reported to hinder STING activation by 4-HNE modification, which inhibits its translocation from the endoplasmic reticulum (ER) to Golgi [18]. Considering the significant impact of stress/CORT on lipid peroxidation observed in our experimental setting, we investigated the effect of CORT exposure in vitro or restraint stress in vivo on this antiviral innate immunity signaling. Cell fraction analysis revealed that CORT induced the retention of STING on the ER (Fig. 4a), while the immunoprecipitation assay suggested that

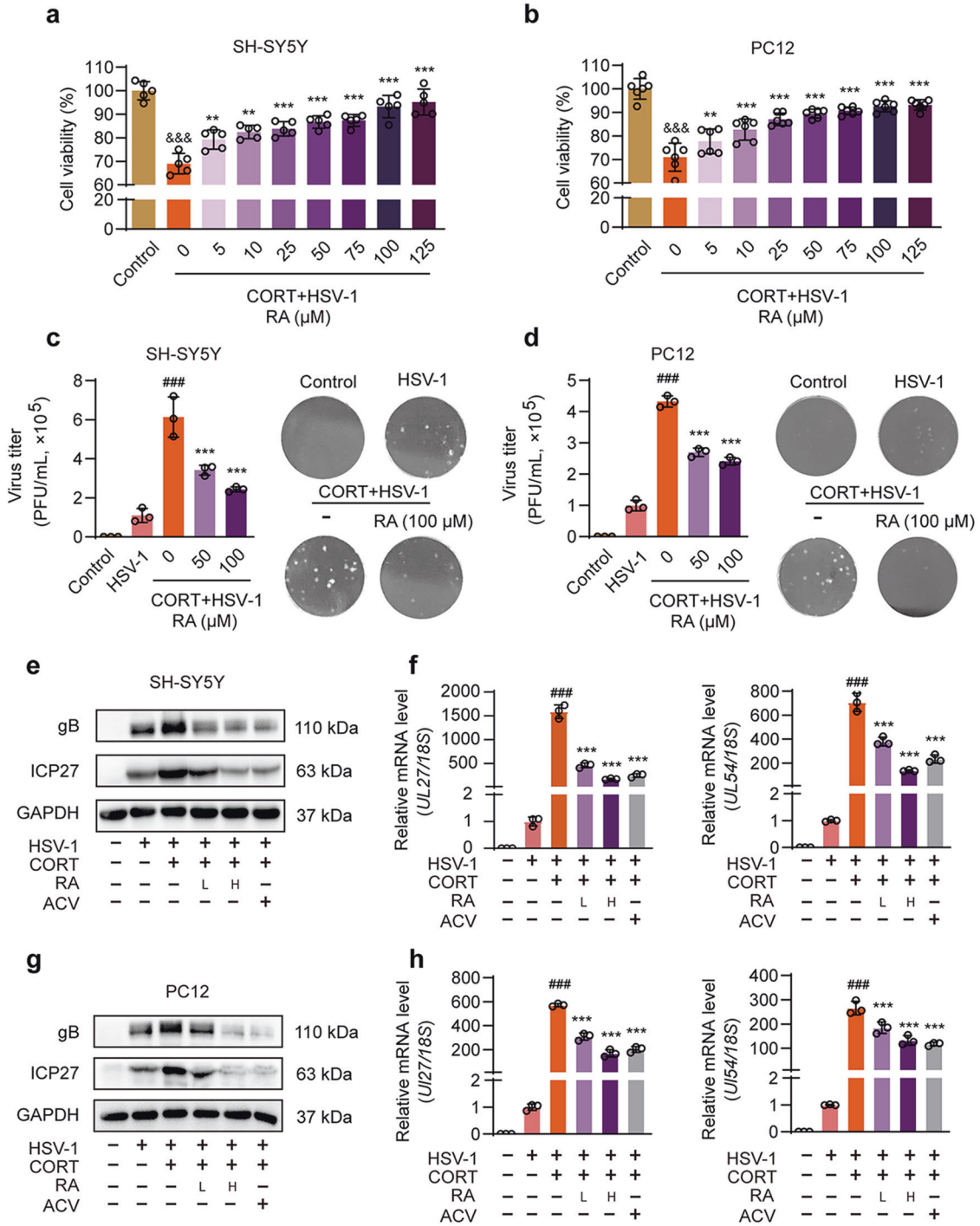

Fig. 2 RA treatment reduces CORT-induced viral susceptibility in neurons. a, **b** The cell viability of SH-SY5Y cells and PC12 cells was determined by MTT assay ($n = 5$ or 6). **c**, **d** Viral titers were detected by the plaque assay and quantified ($n = 3$). **e** Protein expression of gB and ICP27 in SH-SY5Y cells was measured by Western blot. **f** Gene expression of *UL27* and *UL54* in SH-SY5Y cells was measured by qRT-PCR ($n = 3$). **g** Protein expression of gB and ICP27 in PC12 cells was measured by Western blot. **h** Gene expression of *Ul27* and *Ul54* in PC12 cells was measured by qRT-PCR ($n = 3$). HSV-1 (MOI = 1, 24 h), CORT (50 μM, 48 h). Data were presented as mean ± SD. $^{\&\&\&}P < 0.001$ vs. the control group; $^{\#\#\#}P < 0.001$ vs. the HSV-1 group; $^{**}P < 0.01$, $^{***}P < 0.001$ vs. the HSV-1 + CORT group.

CORT treatment led to a considerable increase in the level of 4-HNE-conjugated STING level (Fig. 4b). RA treatment was found to block the retention of STING on the ER and reduce the diminished 4-HNE modification of STING (Fig. 4a, b). However, it did not affect the expression of STING protein and mRNA (Supplementary Fig. S3c, S3d).

Furthermore, we determined type I IFN signaling downstream of STING. As expected, the activation of TBK1/IRF3/IFN-β in response to HSV-1 infection was suppressed by CORT, presented by the reduced level of IFN-β (mRNA in Fig. 4c, protein in Fig. 4f, g), as well as the impeded phosphorylation of TBK1 and IRF3. Similarly, mice subjected to restraint stress displayed a weakened

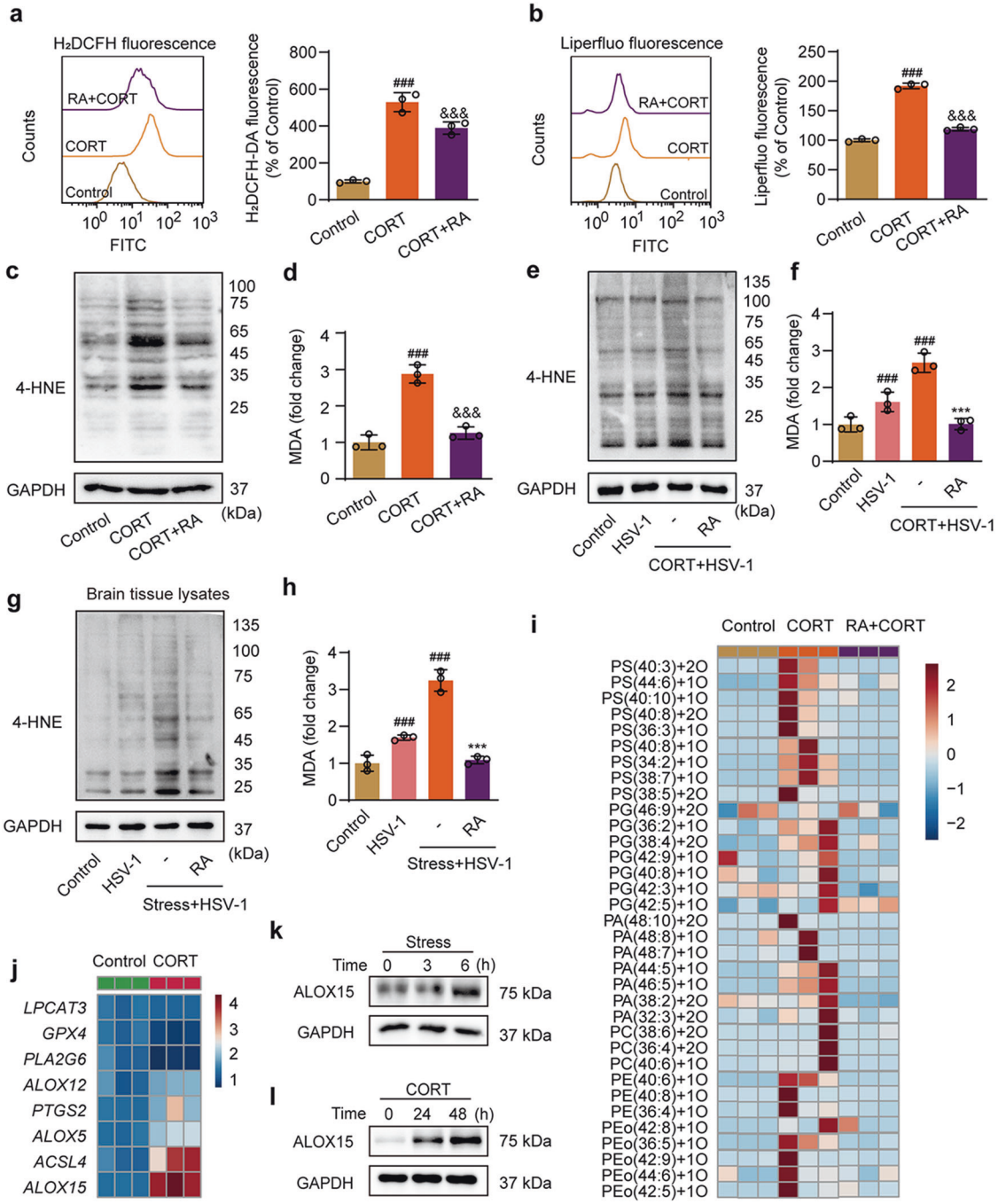

Fig. 3 RA attenuates stress/CORT-induced lipid peroxidation. a, **b** SH-SY5Y cells were stained with H_2DCFH and Liperfluo, respectively, to measure the levels of total ROS and lipid ROS by flow cytometry ($n = 3$). **c**, **e**, **g** The level of 4-HNE-modified proteins was analyzed by Western blot in SH-SY5Y cells in the absence of viruses, in the presence of viruses, and in brain tissues of virus-infected mice. **d**, **f**, **h** The content of MDA was detected in SH-SY5Y cells in the absence of the virus, in the presence of viruses, and in brain tissues of virus-infected mice ($n = 3$). **i** Heatmap indicates the changes of different oxPLs in SH-SY5Y cells in the presence and absence of RA or CORT ($n = 3$). PA Phosphatidic acid, PC Phosphatidylcholine; PG Phosphatidylglycerol, PS Phosphatidylserine, PE Phosphatidylethanolamine. **j** SH-SY5Y cells were pretreated with CORT for 48 h. The gene expression of lipid peroxidation-related proteins was detected by qRT-PCR assay ($n = 3$). **k, l** ALOX15 protein expression was determined by Western blot in the brain tissues of stressed mice and in CORT-treated PC12 cells. CORT: 50 μM, 48 h; RA :100 μM, 48 h. Data are expressed as mean ± SD. $^{###}P < 0.001$ vs. the control group; $^{&&&}P < 0.001$ vs. the CORT group; $^{***}P < 0.001$ vs. the CORT/stress + HSV-1 group.

TBK1/IRF3/IFN-β response to HSV-1 in the brain tissues (mRNA in Fig. 4e, protein in Fig. 4g). In comparison, CORT and stress-blunted innate immunity in vivo and in vitro was identically rescued by RA treatment (Fig. 4a–g). Collectively, all these results infer that RA licenses STING-mediated innate immunity to HSV-1 by maintaining redox homeostasis (Fig. 4h).

ALOX15 is a direct target of RA in inhibiting lipid peroxidation and virus susceptibility

Given the inhibitory effect of RA on lipid peroxidation, we determined the impact of RA treatment on the lipoxygenase ALOX15. Although RA failed to decrease stress/CORT-induced expression of ALOX15 in vivo (Supplementary Fig. S4a) and in vitro (Supplementary Fig. S4b),

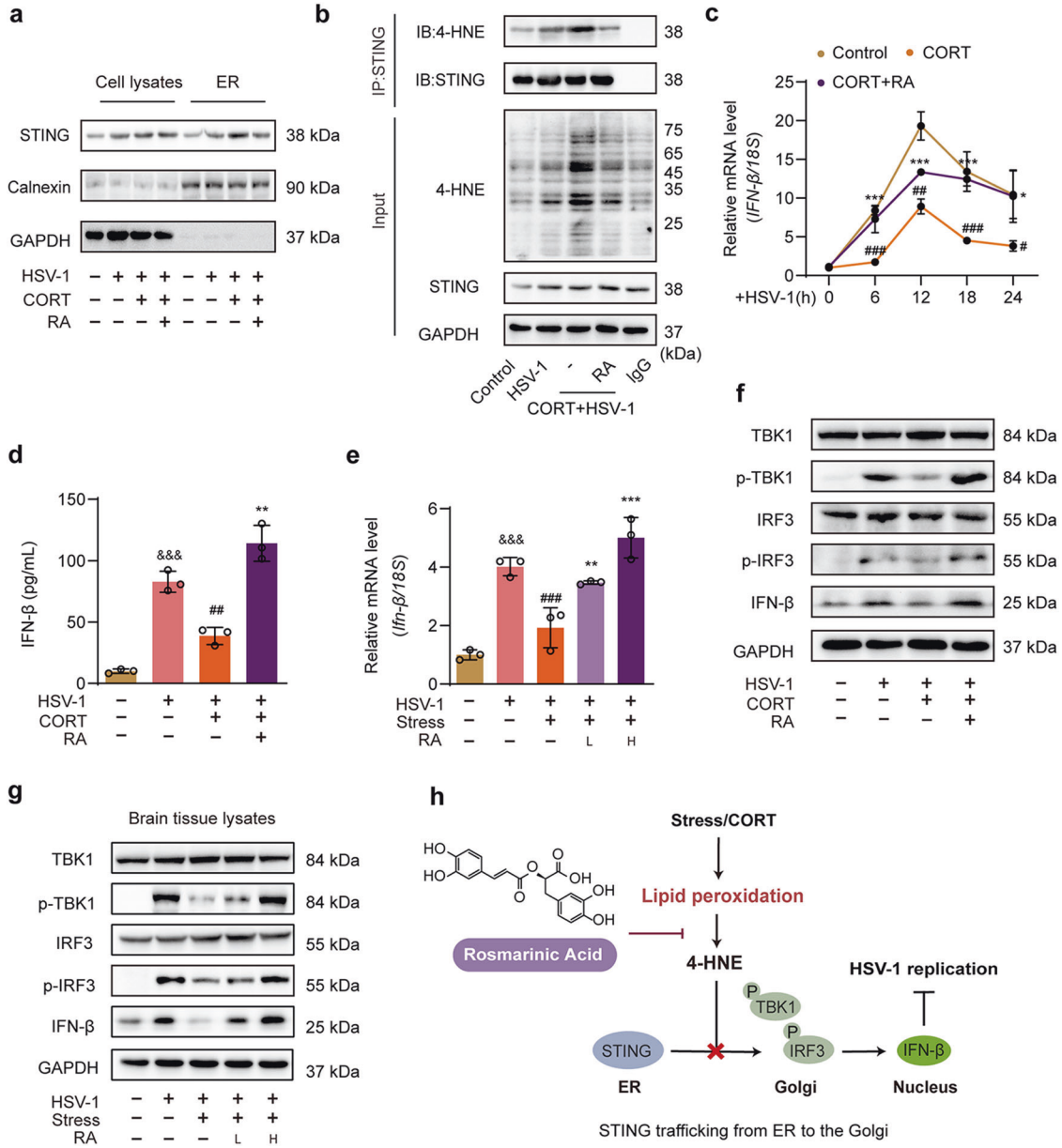

Fig. 4 RA hinders 4-HNE modification of STING antiviral innate immunity. a Immunoblot analysis of STING from the total cell lysates and ER fraction of infected SH-SY5Y cells. Calnexin was used as the ER marker. **b** Immunoprecipitation analysis of 4-HNE modification of STING in CORT-treated SH-SY5Y cells at 24 h post HSV-1 infection. **c** qRT-PCR analysis of *IFN-β* mRNA level in SH-SY5Y cells pretreated with CORT (50 μM) and RA (100 μM) for 48 h, followed by HSV-1 infection for the indicated periods ($n = 3$). **d** IFN-β production determined by ELISA in CORT-treated SH-SY5Y cells at 24 h post-infection ($n = 3$). **e** On day 14 post-virus exposure, *Ifn-β* mRNA in the brain tissues of mice was assessed by qRT-PCR ($n = 3$). **f**, **g** Protein expression of TBK1, p-TBK1, IRF3, p-IRF3, and IFN-β in SH-SY5Y cells and brain tissues. **h** Schematic illustrating the inhibitory effect of RA on stress-provoked 4-HNE modification of STING antiviral innate immunity. RA inhibition of stress/CORT-induced HSV-1 susceptibility. Data are expressed as mean ± SD. $^{\&\&\&}P < 0.001$ vs. the Control group; $^{\#\#}P < 0.01$, $^{\#\#\#}P < 0.001$ vs. the HSV-1 group; $^{*}P < 0.05$, $^{**}P < 0.01$, $^{***}P < 0.001$ vs. the HSV-1 + stress/CORT group.

this compound led to a loss of lipoxygenase activity of ALOX15 in a concentration-dependent manner (Fig. 5a). Notably, RA suppressed the presence of HNE-modified proteins in ALOX15-overexpressing cells (Fig. 5b), reduced the content of MDA (Fig. 5c), and decreased the level of lipid ROS (Fig. 5d).

To confirm the importance of ALOX15 enzymatic properties in CORT-induced HSV-1 susceptibility, we mutated the threonine residue 560 of ALOX15 to methionine (Flag-ALOX15-T560M), resulting in a near total loss of lipoxygenase activity [38, 39]. The mutated ALOX15 did not exacerbate HSV-1 replication like its wild-type form, as evidenced by unaltered viral protein (Fig. 5e) and gene (Fig. 5f, g) expression in CORT-treated SH-SY5Y cells. Furthermore, by taking advantage of molecular docking, we confirmed that RA directly interacts with the residues 361-His and 366-His of ALOX15 (Fig. 5h). This finding was also guaranteed by microscale thermophoresis analysis (MST, Fig. 5i) and cellular thermal shift assay (CETSA, Fig. 5j). Altogether, these data illustrate that the effect of RA on CORT-induced lipid peroxidation and HSV-1 susceptibility is owing to its direct inhibitory effect on ALOX15 catalytic activity.

Alox15 knockout eliminates the effect of RA on stress-augmented HSV-1 susceptibility

To provide more compelling in vivo evidence, we exposed *Alox15* knockout mice to restraint stress and infected them with HSV-1.

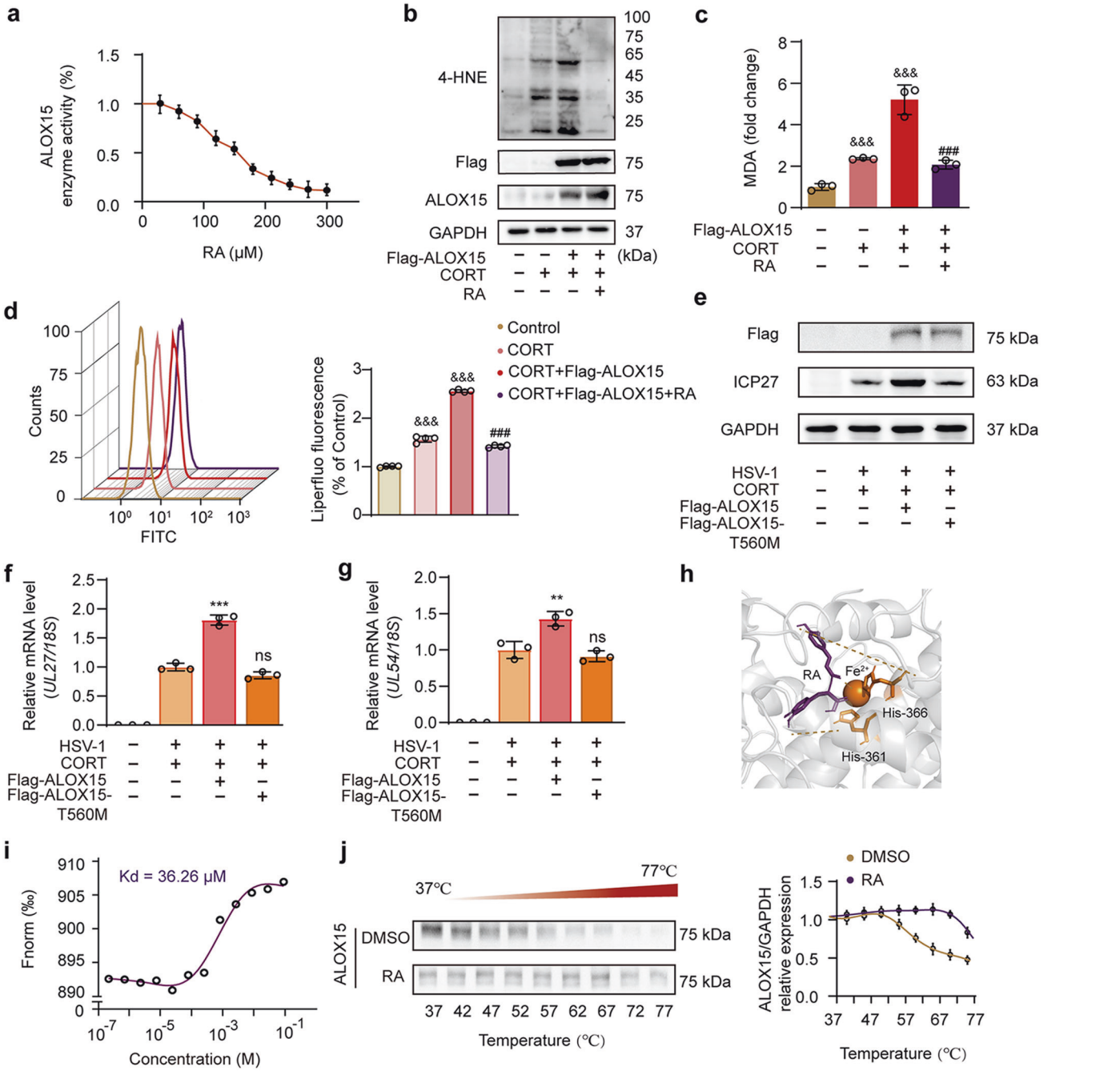

Fig. 5 Identification of ALOX15 as a target of RA in relieving lipid peroxidation and HSV-1 susceptibility. a A concentration-dependent inhibitory effect of RA on ALOX15 enzymatic activity was measured with a commercial kit ($n = 3$). **b**–**d** SH-SY5Y cells were overexpressed with ALOX15 and treated with CORT (50 μM) and RA (100 μM) for 48 h. The level of HNE-modified proteins, the content of MDA, and the amount of Liperfluo-stained lipid ROS were analyzed ($n = 3$). **e**–**g** SH-SY5Y cells were overexpressed with ALOX15 or ALOX15-T560M and treated with CORT (50 μM) and RA (100 μM) for 48 h, followed by HSV-1 infection for 24 h. ICP27 protein level, *UL27*, and *UL54* gene levels were determined ($n = 3$). **h** Molecular docking binding mode of RA and ALOX15. The yellow dotted lines represent hydrogen bonds between RA and the relevant residues of ALOX15. **i**, **j** Binding affinity analysis of RA with ALOX15 was determined by microscale thermophoresis analysis (MST) and cellular thermal shift assay (CETSA) ($n = 3$). Data are expressed as mean ± SD. $^{\&\&\&}P < 0.001$ vs. the Control group; $^{\#\#\#}P < 0.001$ vs. the CORT + Flag-ALOX15 group; $^{**}P < 0.01$, $^{***}P < 0.001$ vs. the HSV-1+CORT group; ns represents no significant.

Our results showed that *Alox15* deficient mice exhibited significantly reduced stress-induced susceptibility to HSV-1, as evidenced by lower levels of eye swell score and virus titers (Fig. 6a, b). Moreover, *Alox15* knockout effectively mitigated the stress-induced suppression of IFN-β production (Fig. 6c). The increase in virus-related genes and proteins provoked by stress was abolished in *Alox15* deficient mice (Fig. 6d–f). Consistently, the induction of lipid peroxidation caused by stress was attenuated in *Alox15* knockout mice (Fig. 6g). In sharp contrast to the effect of RA in wild-type mice, RA displayed little influence on the lipid peroxidation in *Alox15* knockout mice (Fig. 6g). Following in vivo evidence, the stress hormone CORT also failed to promote HSV-1 susceptibility in primary cortical neurons isolated from *Alox15* knockout mice, as indicated by the unaltered viral protein level

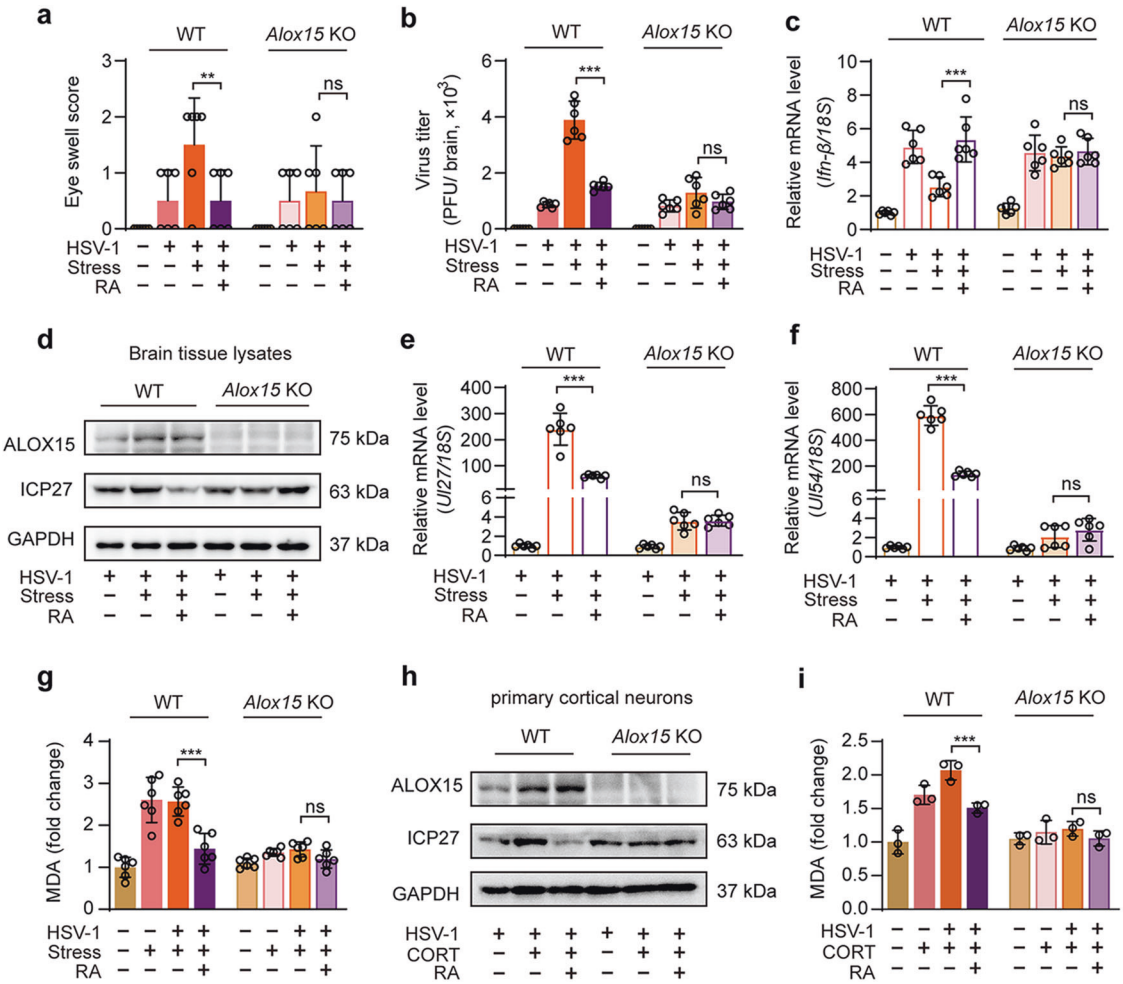

Fig. 6 ***Alox15* deficiency abolishes the effect of RA against stress-enhanced HSV-1 susceptibility. a** WT and *Alox15* knockout mice were treated with stress, HSV-1 exposure and RA administration (23.4 mg·kg^{-1}·d^{-1}, i.g.). Eye swell scores were assessed seven days post-infection using the following criteria: 1, puffy eyelids; 2, puffy eyelids with some crusting; 3, swollen shut with severe crusting; 4, completely swollen shut and crusted over ($n = 6$). **b** On the 14th day post-infection, viral titers in the brain were detected by plaque assay ($n = 6$). **c**–**f** The levels of *Ifn-β* mRNA, ICP27 protein, *Ul27*, and *Ul54* mRNA in brain tissues were detected by qRT-PCR or Western blot ($n = 6$). **g** The content of MDA in the brain tissue was measured by a commercial kit ($n = 6$). **h**, **i** Primary cortical neurons were isolated from *Alox15* knockout (*Alox15* KO) mice and co-treated with CORT (50 μM) and RA (100 μM) for 48 h, followed by viral infection. The levels of ICP27 protein and MDA content were analyzed at 24 h post-infection ($n = 3$). Data are expressed as mean ± SD. $^{**}P < 0.01$, $^{***}P < 0.001$ vs. the HSV-1 + stress/CORT group; ns represents no significance.

(Fig. 6h). In *Alox15*-deficient neurons, the effect of RA against CORT-induced virus susceptibility disappeared. The abrogation of ALOX15 also diminished the generation of lipid peroxidation end-product in CORT-treated neurons (Fig. 6i). These findings obtained from *Alox15* knockout mice provide strong evidence to support the critical role of ALOX15-mediated lipid peroxidation in stress-increased HSV-1 susceptibility (Fig. 7).

DISCUSSION

Current research on disease susceptibility has largely concentrated on identifying susceptible genes involved in particular population segments. However, for most individuals, the cause of susceptibility to diseases can be traced back to other factors, such as emotional stressors [30, 40]. Traditional Chinese medicine has long proposed that emotional stimulation can disrupt the Yin-Yang equilibrium, impacting disease onset, recurrence, and progression [7, 8]. Psychological stress has been acknowledged as a risk factor for viral infections, yet the precise determinants underlying stress-induced HSV-1 susceptibility are still largely unknown. In the present study, by combining phospholipidomics analysis with serial functional validation, we uncover the presence of many oxidized phospholipids in stress/CORT-exposed brain tissues and neurons, leading to active electrophilic aldehydes, which effectively switches off neuronal anti-HSV-1 innate immunity. These findings highlight the significance of lipoxygenase-mediated specific oxidative reactions in stress-induced virus susceptibility, underpinning the interplay between oxidative damage and antiviral innate immunity. Based on this novel pathological mechanism, we illustrate the natural compound RA as a new anti-HSV-1 strategy that targets lipoxygenase ALOX15-mediated phospholipid peroxidation.

Moderate concentration of ROS plays a crucial role in maintaining physiological homeostasis. However, cells enter an oxidative stress state when ROS concentration exceeds the anti-oxidative capacity [36, 41]. The brain is particularly sensitive to redox imbalance due to its high oxygen consumption, limited antioxidant defenses, and lipid-rich composition [11]. In contrast to reports of non-specific oxidative damage in the brain caused by psychological stress [42], we demonstrate that lipoxygenase-catalyzed lipid peroxidation is essential in stress-induced viral infection, with ALOX15 being identified as the principal enzyme

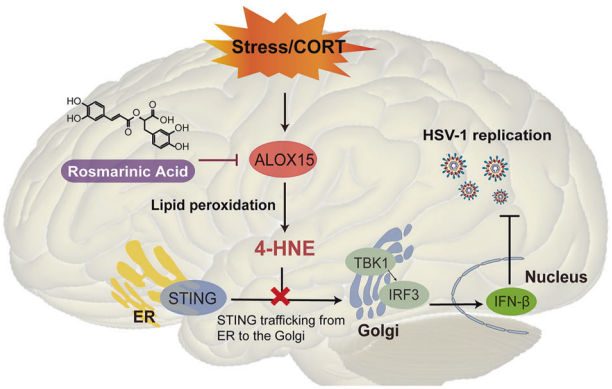

Fig. 7 Schematic illustration depicting the effect and mechanism of RA on stress-induced HSV-1 susceptibility. CORT provokes ALOX15-dependent oxidative stress response in the brain in response to psychological stress. The redox imbalance results in an accumulation of oxidized phospholipids, leading to the generation of 4-HNE in neurons. The innate immunity regulator STING is modified by 4-HNE conjunction, thus inhibiting its trafficking from the ER to the Golgi complex and blocking subsequent innate immune responses against HSV-1. The naturally occurring ALOX15 inhibitor attenuates stress-augmented HSV-1 infection by prohibiting stress-triggered lipid peroxidation from recovering STING-mediated neuronal innate immunity.

involved. In response to stress, ALOX15 was robustly induced, exacerbating the accumulation of lipid peroxidation and augmenting HSV-1 infection in neurons. Conversely, *Alox15* deletion was found to limit stress-induced lipid peroxidation and, thus, increase HSV-1 resistance.

Neurons are known to be the site of lifelong latency of HSV-1 and represent a crucial target for long-term suppressive therapy or viral clearance [43]. In addition to professional immune cells, certain types of pattern recognition receptors (PRRs) are also highly expressed in neurons to initiate a prompt immune response to eliminate pathogens in the central nervous system [44, 45]. For instance, neuronal TLR3 has been reported to recognize and activate during rabies viral infection [46]. The innate immune regulator STING has been shown to play a crucial role in eliciting immunological responses in neurons exposed to the Japanese encephalitis virus [47]. Additionally, a recent study has identified the antinociception role of STING-mediated type I interferon signaling in sensory neurons [48]. Although a clear relationship between GPX4 deficiency-caused lipid peroxidation and STING-mediated antiviral immunity has been well established in professional immune cells [18], our study provides further evidence in neurons by delineating the map among stress, ALOX15-induced redox imbalance, and HSV-1 susceptibility. Our findings may establish the ALOX15-STING axis as a critical regulator of neuronal innate immunity and offer a promising new target for treating HSV-1 infection.

HSV-1 is a common cause of life-threatening encephalitis worldwide [4]. However, prolonged use of anti-herpetic drugs can lead to the emergence of drug-resistant strains and adverse side effects [49]. Traditional medicines and their active components have been shown to effectively combat viral infections with few side effects and low toxicity [50, 51]. RA, which can be isolated from over 160 plants belonging to *Lamiaceae*, *Boraginaceae*, and *Apiaceae* [52], has been discovered to exhibit antiviral properties against several types of viruses, including SARS-CoV-2 [53] and human immunodeficiency virus [54]. Despite this, RA's anti-HSV-1 activity and mechanism have yet to be explored. In this study, by utilizing stress/CORT-established HSV-1 susceptibility models, we uncovered that RA attenuated stress-augmented HSV-1 infection-related eye symptoms and virus replication. The protective effect of RA was abolished in *Alox15* knockout mice. Mechanistically, RA displayed a remarkable inhibitory activity of ALOX15 and reversed CORT-provoked lipid peroxidation, thereby prohibiting the 4-HNE modification of STING and restoring neuronal innate immunity.

In conclusion, the present study utilized in vivo and in vitro models of stress-induced HSV-1 susceptibility to demonstrate the significance of lipid peroxidation in stress-impeded antiviral innate immunity in neurons. The study also discovered that RA is a naturally occurring inhibitor of ALOX15 and provides in vivo and in vitro proof of its anti-HSV-1 effectiveness. These findings offer new perspectives into the pathogenesis of HSV-1 susceptibility and open a new direction for developing novel strategies for HSV-1 infection.

ACKNOWLEDGEMENTS

This study was partly supported by the Natural Science Foundation of Guangdong (2023B1515040016 and 2021B1515120023), the National Natural Science Foundation of China (Grant numbers 82125038, 82274123 and 82174054), the Local Innovative and Research Teams Project of Guangdong Pearl River Talents Program (2017BT01Y036), the Innovation Team Project of Guangdong Provincial Department of Education (2020KCXTD003) and GDUPS (2019), and the National Key Research and Development Program of China (2022YFC0867400). The authors (Rong-rong He and Yi-fang Li) also gratefully acknowledge the support of the K.C. Wong Education Foundation.

AUTHOR CONTRIBUTIONS

YFL, RRH, and HK conceived and designed the research. JYW, XXC, XHW, and HEY performed the experiments. JYW, XXC, and XHW contributed to the acquisition and analysis of the data. JYW and SHOY prepared figures, tables, and the manuscript. YPW, WYS, LL, WJD. FH, XXS, and HK partly advised the research. YFL, RRH, and SHOY revised and approved the manuscript. All of the authors have approved the final manuscript.

ADDITIONAL INFORMATION

Supplementary information The online version contains supplementary material available at https://doi.org/10.1038/s41401-023-01095-6.

Competing interests: The authors declare no competing interests.

REFERENCES

1. Marcocci ME, Napoletani G, Protto V, Kolesova O, Piacentini R, Li Puma DD, et al. Herpes simplex virus-1 in the brain: the dark side of a sneaky infection. Trends Microbiol. 2020;28:808–20.
2. Singh N, Tscharke DC. Herpes simplex virus latency is noisier the closer we look. J Virol. 2020;94:e01701-19.
3. De Chiara G, Piacentini R, Fabiani M, Mastrodonato A, Marcocci ME, Limongi D, et al. Recurrent herpes simplex virus-1 infection induces hallmarks of neurodegeneration and cognitive deficits in mice. PLoS Pathog. 2019;15:e1007617.
4. Piret J, Boivin G. Immunomodulatory strategies in herpes simplex virus encephalitis. Clin Microbiol Rev. 2020;33:e00105-19.
5. Bello-Morales R, Andreu S, Lopez-Guerrero JA. The role of herpes simplex virus type 1 infection in demyelination of the central nervous system. Int J Mol Sci. 2020;21:5026.
6. Li W, Luo Z, Yan CY, Wang XH, He ZJ, Ouyang SH, et al. Autophagic degradation of PML promotes susceptibility to HSV-1 by stress-induced corticosterone. Theranostics. 2020;10:9032–49.
7. Pan MH, Zhu SR, Duan WJ, Ma XH, Luo X, Liu B, et al. "Shanghuo" increases disease susceptibility: Modern significance of an old TCM theory. J Ethnopharmacol. 2020;250:112491.
8. Yan C, Luo Z, Li W, Li X, Dallmann R, Kurihara H, et al. Disturbed Yin-Yang balance: Stress increases the susceptibility to primary and recurrent infections of herpes simplex virus type 1. Acta Pharm Sin B. 2020;10:383–98.
9. Mora F, Segovia G, Del Arco A, de Blas M, Garrido P. Stress, neurotransmitters, corticosterone and body-brain integration. Brain Res. 2012;1476:71–85.
10. Wu Y, Luo X, Zhou Q, Gong H, Gao H, Liu T, et al. The disbalance of LRP1 and SIRPalpha by psychological stress dampens the clearance of tumor cells by macrophages. Acta Pharm Sin B. 2022;12:197–209.
11. Bouayed J, Rammal H, Soulimani R. Oxidative stress and anxiety: Relationship and cellular pathways. Oxid Med Cell Longev. 2009;2:63–7.

12. Guo H, Zheng L, Xu H, Pang Q, Ren Z, Gao Y, et al. Neurobiological links between stress, brain injury, and disease. Oxid Med Cell Longev. 2022;2022:8111022.
13. Diniz BS, Mendes-Silva AP, Silva LB, Bertola L, Vieira MC, Ferreira JD, et al. Oxidative stress markers imbalance in late-life depression. J Psychiatr Res. 2018;102:29–33.
14. Lim DW, Park J, Jung J, Kim SH, Um MY, Yoon M, et al. Dicaffeoylquinic acids alleviate memory loss via reduction of oxidative stress in stress-hormone-induced depressive mice. Pharmacol Res. 2020;161:105252.
15. Burtscher J, Copin JC, Rodrigues J, Kumar ST, Chiki A, Guillot de Suduiraut I, et al. Chronic corticosterone aggravates behavioral and neuronal symptomatology in a mouse model of alpha-synuclein pathology. Neurobiol Aging. 2019;83:11–20.
16. Gaschler MM, Stockwell BR. Lipid peroxidation in cell death. Biochem Biophys Res Commun. 2017;482:419–25.
17. Chen X, Kang R, Kroemer G, Tang D. Ferroptosis in infection, inflammation, and immunity. J Exp Med. 2021;218:e20210518.
18. Jia M, Qin D, Zhao C, Chai L, Yu Z, Wang W, et al. Redox homeostasis maintained by GPX4 facilitates STING activation. Nat Immunol. 2020;21:727–35.
19. Zhu H, Zheng C. The race between host antiviral innate immunity and the immune evasion strategies of herpes simplex virus 1. Microbiol Mol Biol Rev. 2020;84:e00099-20.
20. Dahchour A. Anxiolytic and antidepressive potentials of rosmarinic acid: A review with a focus on antioxidant and anti-inflammatory effects. Pharmacol Res. 2022;184:106421.
21. Jheng JR, Hsieh CF, Chang YH, Ho JY, Tang WF, Chen ZY, et al. Rosmarinic acid interferes with influenza virus A entry and replication by decreasing GSK3beta and phosphorylated AKT expression levels. J Microbiol Immunol Infect. 2022;55:598–610.
22. Ali S, Alam M, Khatoon F, Fatima U, Elasbali AM, Adnan M, et al. Natural products can be used in therapeutic management of COVID-19: Probable mechanistic insights. Biomed Pharmacother. 2022;147:112658.
23. Genis-Galvez JM. Role of the lens in the morphogenesis of the iris and cornea. Nature. 1966;210:209–10.
24. Reinert LS, Lopusna K, Winther H, Sun C, Thomsen MK, Nandakumar R, et al. Sensing of HSV-1 by the cGAS-STING pathway in microglia orchestrates antiviral defence in the CNS. Nat Commun. 2016;7:13348.
25. Cardozo FT, Larsen IV, Carballo EV, Jose G, Stern RA, Brummel RC, et al. In vivo anti-herpes simplex virus activity of a sulfated derivative of *Agaricus brasiliensis* mycelial polysaccharide. Antimicrob Agents Chemother. 2013;57:2541–9.
26. Yu Z, Xu J, Liu N, Wang Y, Li X, Pallast S, et al. Mitochondrial distribution of neuroglobin and its response to oxygen-glucose deprivation in primary-cultured mouse cortical neurons. Neuroscience. 2012;218:235–42.
27. Folch J, Lees M, Sloane Stanley GH. A simple method for the isolation and purification of total lipides from animal tissues. J Biol Chem. 1957;226:497–509.
28. Luo X, Gong HB, Gao HY, Wu YP, Sun WY, Li ZQ, et al. Oxygenated phosphatidylethanolamine navigates phagocytosis of ferroptotic cells by interacting with TLR2. Cell Death Differ. 2021;28:1971–89.
29. Wieckowski MR, Giorgi C, Lebiedzinska M, Duszynski J, Pinton P. Isolation of mitochondria-associated membranes and mitochondria from animal tissues and cells. Nat Protoc. 2009;4:1582–90.
30. Poller WC, Downey J, Mooslechner AA, Khan N, Li L, Chan CT, et al. Brain motor and fear circuits regulate leukocytes during acute stress. Nature. 2022;607:578–84.
31. Lee EH, Park JY, Kwon HJ, Han PL. Repeated exposure with short-term behavioral stress resolves pre-existing stress-induced depressive-like behavior in mice. Nat Commun. 2021;12:6682.
32. Luo Z, Liu LF, Jiang YN, Tang LP, Li W, Ouyang SH, et al. Novel insights into stress-induced susceptibility to influenza: corticosterone impacts interferon-beta responses by Mfn2-mediated ubiquitin degradation of MAVS. Signal Transduct Target Ther. 2020;5:202.
33. Valyi-Nagy T, Dermody TS. Role of oxidative damage in the pathogenesis of viral infections of the nervous system. Histol Histopathol. 2005;20:957–67.
34. Protto V, Tramutola A, Fabiani M, Marcocci ME, Napoletani G, Iavarone F, et al. Multiple Herpes Simplex Virus-1 (HSV-1) Reactivations induce protein oxidative damage in mouse brain: novel mechanisms for Alzheimer's disease progression. Microorganisms. 2020;8:972.
35. Ling JX, Wei F, Li N, Li JL, Chen LJ, Liu YY, et al. Amelioration of influenza virus-induced reactive oxygen species formation by epigallocatechin gallate derived from green tea. Acta Pharmacol Sin. 2012;33:1533–41.
36. Hu S, Sheng WS, Schachtele SJ, Lokensgard JR. Reactive oxygen species drive herpes simplex virus (HSV)-1-induced proinflammatory cytokine production by murine microglia. J Neuroinflammation. 2011;8:123.
37. Ishikawa H, Barber GN. STING is an endoplasmic reticulum adaptor that facilitates innate immune signalling. Nature. 2008;455:674–8.
38. Assimes TL, Knowles JW, Priest JR, Basu A, Borchert A, Volcik KA, et al. A near null variant of 12/15-LOX encoded by a novel SNP in ALOX15 and the risk of coronary artery disease. Atherosclerosis. 2008;198:136–44.
39. Schurmann K, Anton M, Ivanov I, Richter C, Kuhn H, Walther M. Molecular basis for the reduced catalytic activity of the naturally occurring T560M mutant of human 12/15-lipoxygenase that has been implicated in coronary artery disease. J Biol Chem. 2011;286:23920–7.
40. Marques-Deak A, Cizza G, Sternberg E. Brain-immune interactions and disease susceptibility. Mol Psychiatry. 2005;10:239–50.
41. Kim HJ, Kim CH, Ryu JH, Kim MJ, Park CY, Lee JM, et al. Reactive oxygen species induce antiviral innate immune response through IFN-lambda regulation in human nasal epithelial cells. Am J Respir Cell Mol Biol. 2013;49:855–65.
42. Wang X, Michaelis EK. Selective neuronal vulnerability to oxidative stress in the brain. Front Aging Neurosci. 2010;2:12.
43. Rosato PC, Leib DA. Neurons versus herpes simplex virus: The innate immune interactions that contribute to a host-pathogen standoff. Future Virol. 2015;10:699–714.
44. Kigerl KA, de Rivero Vaccari JP, Dietrich WD, Popovich PG, Keane RW. Pattern recognition receptors and central nervous system repair. Exp Neurol. 2014;258:5–16.
45. Lin Y, Zheng C. A Tug of war: DNA-sensing antiviral innate immunity and herpes simplex virus type I infection. Front Microbiol. 2019;10:2627.
46. Prehaud C, Megret F, Lafage M, Lafon M. Virus infection switches TLR-3-positive human neurons to become strong producers of beta interferon. J Virol. 2005;79:12893–904.
47. Nazmi A, Mukhopadhyay R, Dutta K, Basu A. STING mediates neuronal innate immune response following Japanese encephalitis virus infection. Sci Rep. 2012;2:347.
48. Donnelly CR, Jiang C, Andriessen AS, Wang K, Wang Z, Ding H, et al. STING controls nociception via type I interferon signalling in sensory neurons. Nature. 2021;591:275–80.
49. Looker KJ, Garnett GP. A systematic review of the epidemiology and interaction of herpes simplex virus types 1 and 2. Sex Transm Infect. 2005;81:103–7.
50. Li W, Wang XH, Luo Z, Liu LF, Yan C, Yan CY, et al. Traditional chinese medicine as a potential source for HSV-1 therapy by acting on virus or the susceptibility of host. Int J Mol Sci. 2018;19:3266.
51. Luo Z, Kuang XP, Zhou QQ, Yan CY, Li W, Gong HB, et al. Inhibitory effects of baicalein against herpes simplex virus type 1. Acta Pharm Sin B 2020;10:2323–38.
52. Guan H, Luo W, Bao B, Cao Y, Cheng F, Yu S, et al. A Comprehensive review of rosmarinic acid: from phytochemistry to pharmacology and its new insight. Molecules. 2022;27:3292.
53. Elebeedy D, Elkhatib WF, Kandeil A, Ghanem A, Kutkat O, Alnajjar R, et al. Anti-SARS-CoV-2 activities of tanshinone IIA, carnosic acid, rosmarinic acid, salvianolic acid, baicalein, and glycyrrhetinic acid between computational and in vitro insights. RSC Adv. 2021;11:29267–86.
54. Bekut M, Brkic S, Kladar N, Dragovic G, Gavaric N, Bozin B. Potential of selected *Lamiaceae* plants in anti(retro)viral therapy. Pharmacol Res. 2018;133:301–14.